

Supporting Information

Baddeley et al. 10.1073/pnas.09089711106

SI Text

Additional Stochastic Self-Assembly Models of RyR Cluster Formation.

A simple model of cluster formation was able to reproduce the observed cluster size distribution (see main text). That model required only few free parameters at the expense of not describing in detail the diffusion of mobile RyRs in the membrane. To show that a model that includes receptor diffusion produces similar results we also constructed a second, more complex model. The model included two RyR populations, a mobile fraction that freely diffuses in the SR membrane, and a fraction of fixed receptors that are bound to (unspecified) anchoring structures. A Monte Carlo simulation was implemented on a 100×100 grid with unit cell size equal to the RyR size (30 nm). Diffusion of mobile receptors was implemented via movement to one of its randomly chosen four neighbouring grid cells per time step, provided that cell was not occupied by another receptor. The diffusion used periodic boundary conditions. New mobile receptors were inserted into the membrane with a probability p_{seed} of $1.3 \cdot 10^{-3}$ per time step. Mobile receptors could become fixed by binding to randomly occurring anchoring proteins (with a probability $p_{fix} = 8 \cdot 10^{-4}$) or by binding to fixed RyRs with which they come into direct contact. RyRs with a single fixed neighbor had a probability of binding of 0.5. Two or more neighbouring RyRs resulted in certain binding. To generate a simulated cluster configuration 200 time steps were performed.

The probability p_{seed} of seeding new receptors was set to $1.3 \cdot 10^{-5}$ for the last 50 steps to simulate the cessation of the major growth phase. Cluster size distributions from 200 runs were pooled to generate cluster size histograms.

Independent support of the idea that the observed cluster size distributions reflects stochastic self-assembly of diffusible receptors was provided by comparison with an analytical model of cluster formation that was recently described in ref. 1. The model assumes that receptors are inserted into the membrane at random locations and diffuse within the membrane until captured by existing immobile clusters. While the model was originally developed for a growing population of bacterial cells the biophysical principles it is based upon are also applicable to the stochastic assembly of RyR clusters in growing heart cells. In the steady state, the probability $p(N)$ of finding a cluster containing N receptors can then under fairly general conditions (which include that the cluster center-to-center distances are large compared to the cluster half-diameter) be approximated by the expression:

$$p(N) = c_1 \exp(-c_2 N + c_3 N \ln(N) - c_4 N (\ln(N))^2)$$

with unknown constants c_1 , c_2 , c_3 , and c_4 (1). We fitted this equation with four free parameters to our observed histograms, noting that histogram frequencies are proportional to $p(N)$ in the limit of large numbers of clusters.

1. Greenfield D, et al. (2009) Self-organization of the *Escherichia coli* chemotaxis network imaged with super-resolution light microscopy. *PLoS Biol* 7:e1000137.

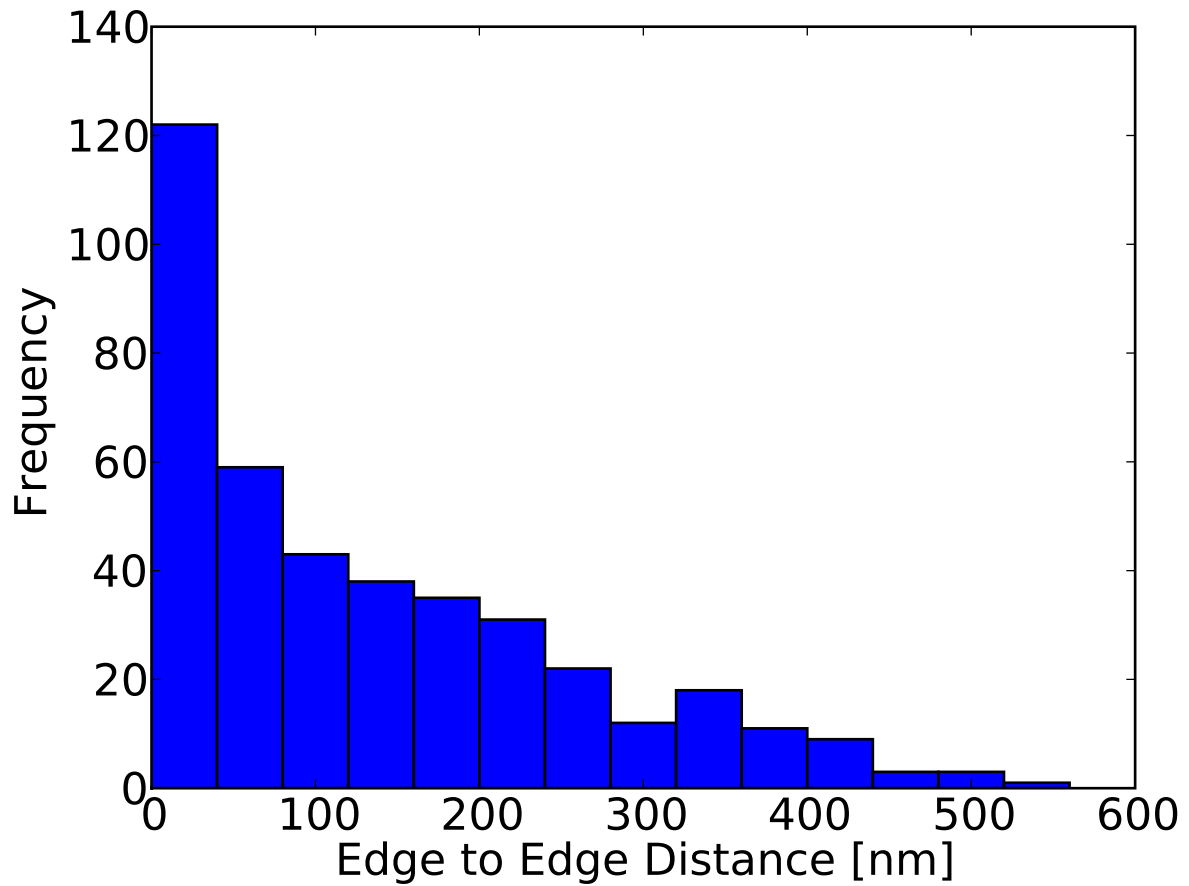


Fig. S1. Edge-to-edge distances between peripheral RyR clusters in a typical cell. This information is complementary to the RyR cluster center-to-center distances and important in determining the likelihood of cross-signaling between clusters during activation. Clusters are close to their nearest neighbors with approximately half of all clusters being within 100 nm of a neighboring site.

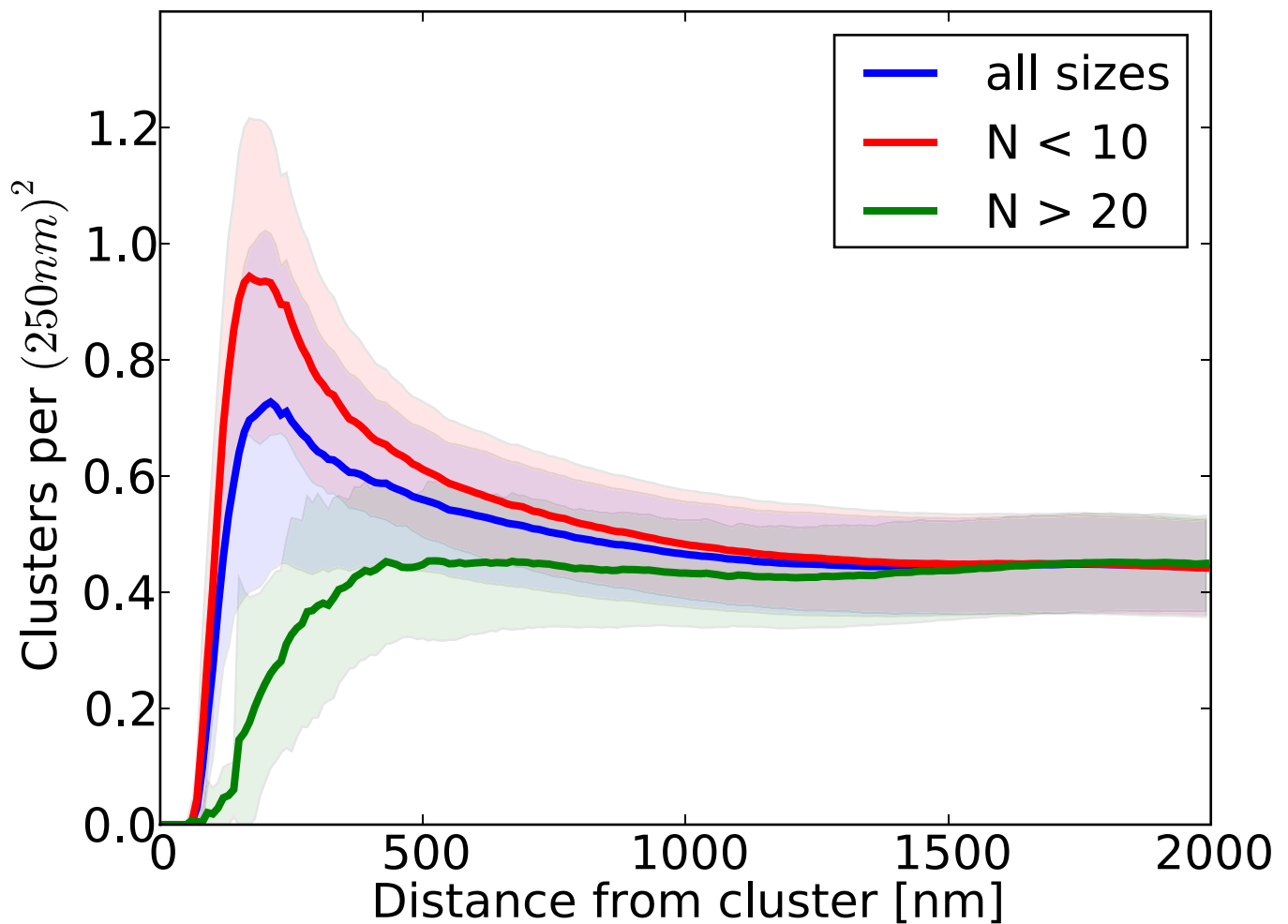


Fig. S2. The density of neighboring clusters as a function of the distance from a cluster center. The low values at small distances can be largely attributed to size exclusion effects. For a uniform distribution of clusters, the density would then be expected to rise to a constant level and remain there. The observed distribution, however, peaks just above the cluster size, indicating a nonuniform distribution in which clusters are “bunched” together, i.e., it is more likely to find a cluster close to another one than far away from it. Looking at the small ($N_{\text{RyR}} < 10$) and large ($N_{\text{RyR}} > 20$) clusters separately shows that this bunching is most pronounced for smaller clusters. The right shift of the initial rise in the density of larger clusters can be attributed to the larger excluded area of these clusters.

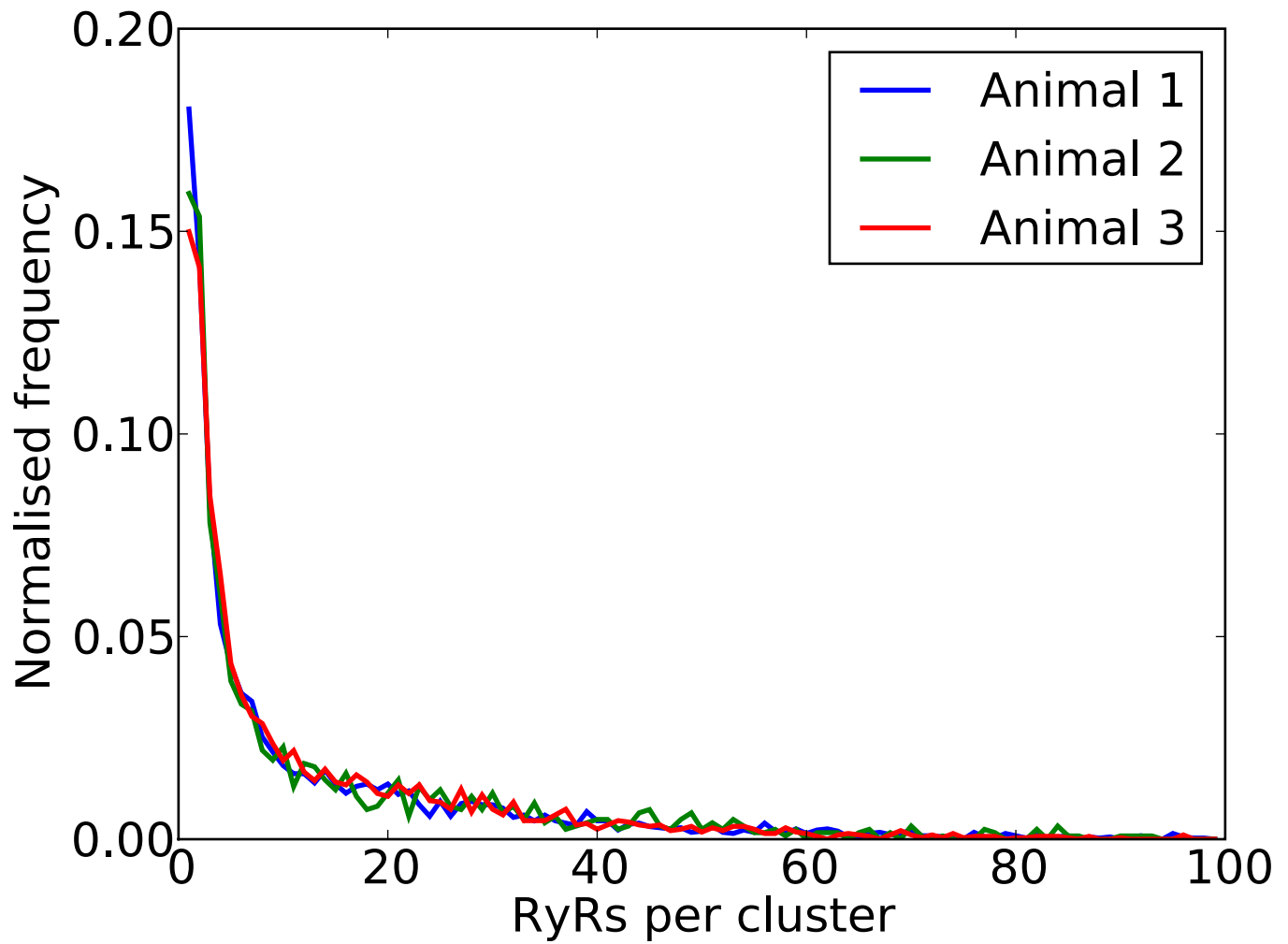


Fig. S3. Animal to animal variability in RyR cluster size. We observed very little variability in RyR cluster size between animals as illustrated by the close agreement in the cluster size distribution observed for different animals. The mean cluster sizes in the three animals were 13.6 ($n = 11$ cells), 14.0 ($n = 4$ cells), and 13.2 ($n = 7$ cells) RyRs per cluster, respectively.

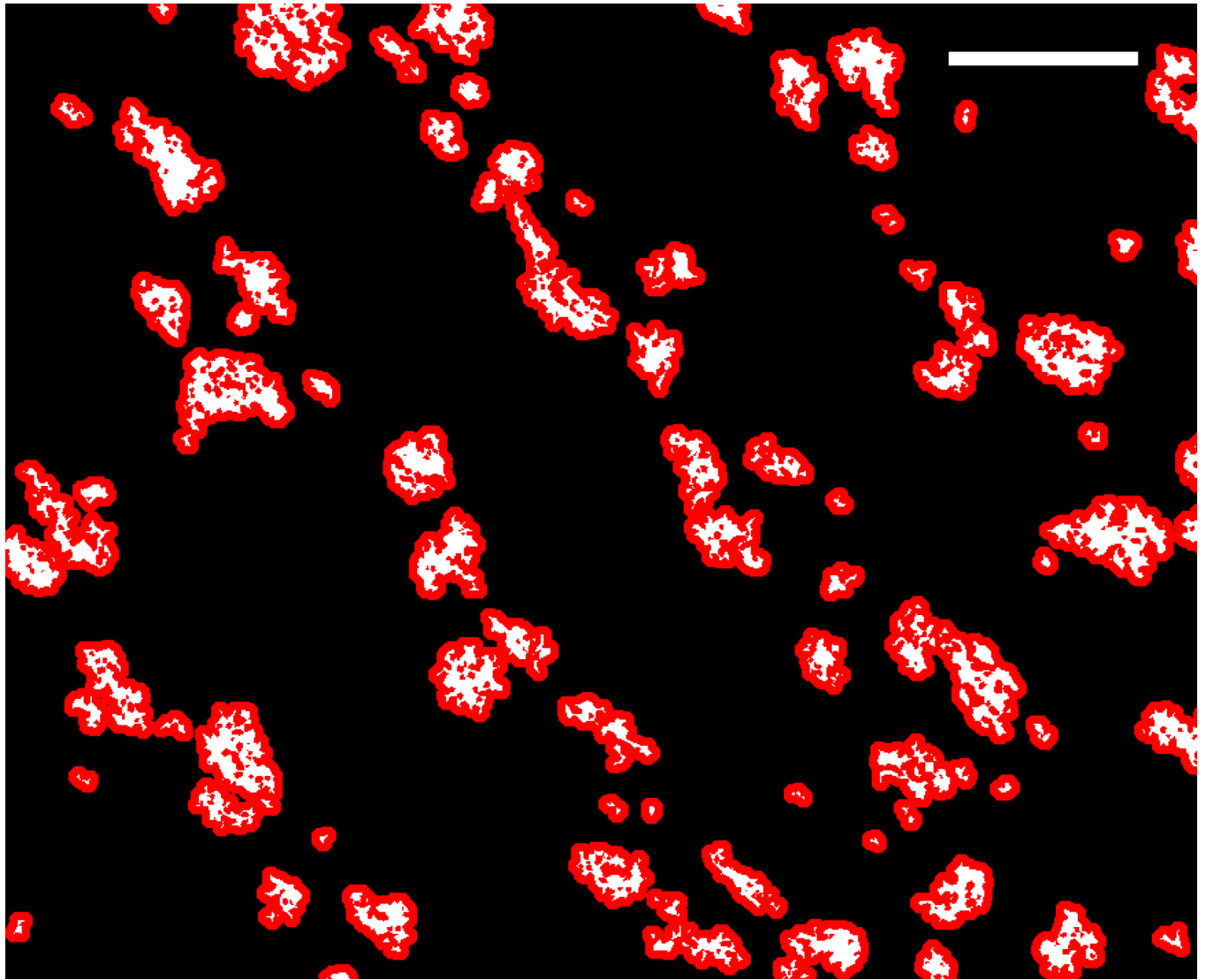


Fig. S4. The concept of RyR superclusters. This image shows detected clusters (white) with a 50-nm “halo” (red) indicating an “area of influence” around each cluster. This is based on the idea that within ≈ 100 nm of an active cluster $[Ca^{2+}]$ is expected to be high enough ($>10 \mu M$) to induce RyR activation. Contiguous regions of red thus represent groups of clusters whose edge to edge distances are <100 nm. These groups might be expected to act functionally as one supercluster (possibly with stochastic recruitment among members) in response to a trigger in any of the constituent clusters. (Scale bar, $1 \mu m$.)

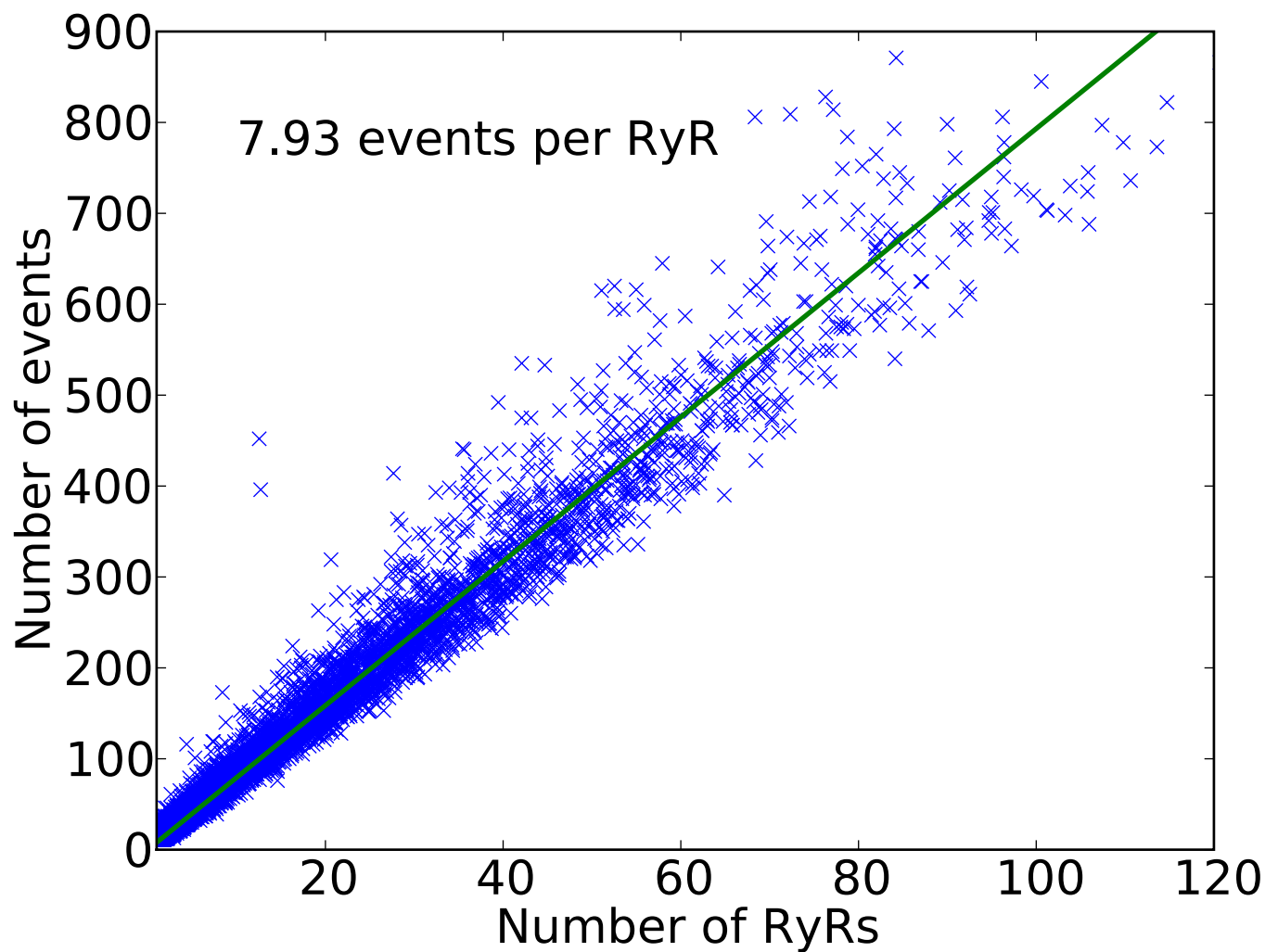


Fig. S6. Relationship between RyRs and detected event numbers. When the number of single molecule events observed within a cluster is plotted against the number of estimated RyRs a strong linear correlation is observed with a slope of approximately 7.9 events/RyR. A linear relationship between the amount of labeling and cluster size is to be expected, and supportive of our segmentation and size estimation method. The number of events per RyR (yielding a single RyR signal to noise of ≈ 2.8) is consistent with our ability to obtain reliable estimates of cluster size.